Effect of low frequency burner vibrations on the characteristics of jet diffusion flames

C. Kanthasamy, Vasudevan Raghavan* and K. Srinivasan

Department of Mechanical Engineering, Indian Institute of Technology Madras, Chennai, INDIA - 600036

Received June 3, 2011; Accepted June 15, 2011

ABSTRACT

Mechanical vibrations introduced in diffusion flame burners significantly affect the flame characteristics. In this experimental study, the effects of axial vibrations on the characteristics of laminar diffusion flames are investigated systematically. The effect of the frequency and amplitude of the vibrations on the flame height oscillations and flame stability is brought out. The amplitude of flame height oscillations is found to increase with increase in both frequency and amplitude of burner vibrations. Vibrations are shown to enhance stability of diffusion flames. Although flame lifts-off sooner with vibrations, stability of the flame increases.

1. INTRODUCTION

Diffusion flames are observed in several applications and are safer in many aspects. In a few applications such as in burners used in moving air/ground vehicles, the diffusion flame burner system is subjected to mechanical vibrations. The basic characteristics of the diffusion flames are affected depending upon the amplitude and frequency of these vibrations. Oscillating diffusion flames have been widely studied by several researchers. These studies investigate the characteristics of naturally flickering diffusion flames, as well as diffusion flames under forced acoustic oscillations. It is evident from the literature that flame oscillations are mainly achieved by acoustic excitations. To the knowledge of the authors, the effect of mechanical vibrations on burners is absent in the literature. This forms the motivation for this work. Some relevant studies on jet and flame oscillations using acoustic excitations are presented in the following paragraphs.

The effect of acoustic excitations on the cold-flow jet characteristics was studied by Zaman et al. [1]. Hotwire anemometry was used to measure and conclude that the

*Corresponding author: E-mail: raghavan@iitm.ac.in

near-nozzle velocity field is significantly affected by the controlled acoustic excitations. The effect of jet exit flow pattern on mixing process was described by Nathan et al. [2] and the possible approaches to enhance large scale oscillations in non-reacting jets were discussed. The reductions in the peak temperature and in NOx emissions reduction were observed when burner exit flow was excited. Albers et al. [3] used quantitative rainbow schlieren deflectometry to characterize the flickering of hydrogen-air flame and its effect on the flow-field. Hamins et al. [4] studied the pulsation frequency of diffusion flames of both gaseous and liquid fuels. They reported the effect of exit velocity and the burner diameter on the pulsation frequency of non-premixed flames. Grant et al. [5] showed that the low frequency oscillations, which are characteristic of small scale flames, dominate even in the turbulent flame regime at higher flow rates.

Aguerre et al. [6] studied counter-flow diffusion flames with sinusoidal velocity variations at the burner exit, both experimentally and numerically. It was reported that the flame becomes insensitive to the vibrations at high frequencies. Mohammad et al. [7] performed experiments as well as numerical simulations of acoustically excited laminar diffusion flames. They observed that the oscillations induced in laminar jet flames assist to bridge the gap between laminar and turbulent combustion processes. They focused on the acoustic oscillations having a frequency of 20 Hz. The responses of the flame in terms of the oscillations in flame shape, structure and heat release, to the acoustic oscillations were found to be different in increasing and decreasing exit velocity portions of a cycle. They also showed that there is a phase change between the input oscillations and the corresponding response in the flame oscillations. In a similar work, Dworkin et al. [8] studied acoustically forced, time varying, laminar methane-air co-flow diffusion flames. They used Rayleigh scattering and Raman scattering methods and presented the variations in isotherms and species profiles for input oscillations at 20 Hz. Several researchers [9–13] have studied acoustically excited flames and the effect on soot and emission dynamics.

Excited flames in the turbulent regime and in lifted diffusion flame regimes have also been studied by researchers. Chao et al. [14] conducted experiments on the characteristics of the turbulent lifted flames with acoustic excitations. They showed the importance of the large scale coherent vortical structures on the stability of the lifted flames in the hysteresis region. Hot wire anemometry data was provided to support their observations on entrainment rates. Takahashi et al. [15, 16] and Pitts [17, 18] provided the understanding of lifting mechanism and the importance of flow conditions in lifting of turbulent flames. Peters [19], Guttenfelder et al. [20] and Mansour et al. [21] reported the relationship between mixing enhancement and preheat zone thickness by their observations on mixing length scales and corresponding thickening and thinning of the preheat region. Weinberg [22] presented the relationship between the intensity of shadowgraph and the flame structure.

Markstein [23] qualitatively studied the effect of flow disturbances on the premixed flame characteristics. The effects of both acoustic and structural disturbances on flame shapes were studied. A vibrating wire was kept in flame area

and the changes in the flame front shapes were studied in detail using spark shadowgraph and schlieren images. Peterson and Emmons [24] systematically studied the stability of laminar premixed flames stabilized on a wire. The importance of Markstein curvature parameter on the stability of flames was emphasized. The velocity fluctuations observed in laminar flames were termed flame induced turbulence.

As evident in the literature review above, there is scarcely any reference of studies on mechanical excitations of flames. With this motivation, experiments have been designed to impart harmonic mechanical oscillations to laminar diffusion flame burners. Overall flow features such as jet entrainment, flame structure and evolution are expected to be modified as a result of mechanical excitations to the burner. The details of the experimental setup and procedure are detailed below.

2. EXPERIMENTAL SETUP AND PROCEDURE

2.1. Experimental setup

The schematic of the experimental setup is shown in Fig. 1(a). A tubular brass burner [Fig. 1(b)] of 4 mm internal diameter with 1 mm wall thickness is fitted to a settling chamber. The burner is mounted over a small vibration exciter (B&K 4808). The desired sinusoidal signals are generated using a signal generator (Tektronix AFG 320) and passed through a power amplifier (B&K 2719) and then sent to the exciter. The displacement amplitude of the burner-mount vibrations, as a function of input voltage amplitude, is calibrated using an IEPE accelerometer (B&K; Model 4513-001) of sensitivity 100 mV/g. Methane is supplied to the burner through a stainless steel pre-calibrated mass flow controller (Aalborg; Model GFC17-07). The accuracy of mass flow rate measured is within ±1.5% and repeatability is ±0.5%.

A shadowgraph arrangement is set up to visualize the flame as static images and high speed videos. A projector lamp is used as light source, with a translucent paper as a cover to diffuse the light for required intensity. The light beam is then passed through a slit to produce a point source. A biconvex lens is used as collimator. The collimated light beam is captured by a high speed camera from a suitable position, after the light ray passes through the flame region.

Hotwire anemometry is performed to investigate the cold flow entrainment spectra near the burner exit. A two dimensional, constant temperature hotwire anemometer (DANTEC Mini CTA 54T30) is used with miniature type probe (wire diameter 5 μm).

2.2. Experimental procedure

In order to excite the flames, low frequency vibrations in the range of 10 Hz–30 Hz, with amplitudes ranging from 0.25 mm–1 mm are imparted to the burner. The amplitude of vibration is limited to 1 mm, which is the maximum possible for the 30 Hz frequency case, due to the power restriction of the exciter and the total weight of the burner and mounting. Typical burner oscillation spectra are shown in Fig. 2 for various frequencies with constant amplitude of 1 mm. These spectra are derived from the signals obtained from the accelerometer mounted on the burner base. This shows

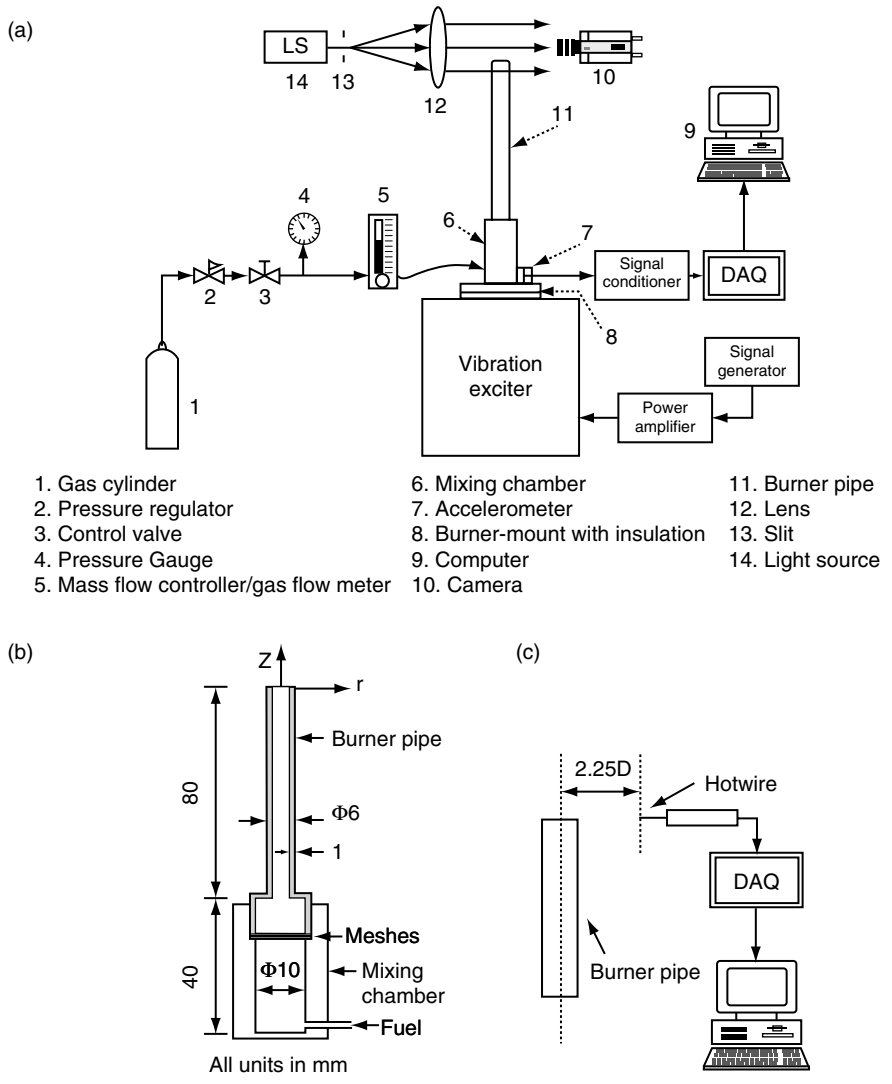

Figure 1: Schematic of (a) the experimental setup (b) the burner and (c) hotwire location.

that the oscillations in acceleration follow the input frequency predominantly. Required methane flow rate is set on the mass flow controller and the fuel is ignited near the burner exit. The exciter is switched on and the required frequency and amplitude of vibration are set. After the burner is set to steady vibrations, direct flame videos using high speed camera are recorded. The frame rate is set as 300 fps. Images are extracted from the high-speed video. The acquired images are processed using

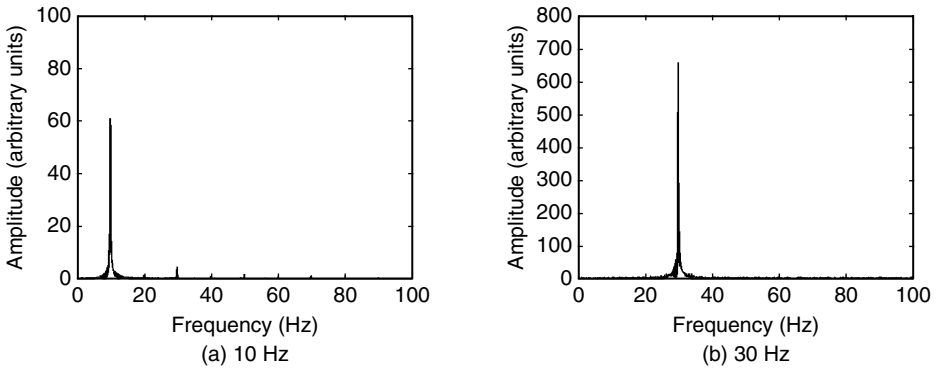

Figure 2: Acceleration spectra for exciter vibrations for 1 mm amplitude.

image processing software - ImageJ [25], for conversion to grayscale, edge detection, etc. The edge detected text images are used to estimate the maximum vertical location of the edge, which corresponds to the flame height (L_f). These calculations are performed using MATLAB software. The images are acquired for 2 s (600 frames) and are processed for each case to encompass a minimum of 20 cycles. The time interval between the frames is 3.33 ms. The mean flame height (L_{mean}) is also calculated by time averaging the instantaneous flame heights.

3. RESULTS AND DISCUSSION

3.1. Fluctuations in air entrainment

Hotwire anemometry is performed near the burner exit at the burner exit plane (z = 0) at a radial location of r = 2.25D from the axis of the burner [see Fig. 1(c)]. Single point measurements are made following the work of Valk [26]. These entrainment velocity measurements are performed only in cold air jet flows in order to avoid placing the hotwire in the vicinity of flames. In these measurements, the Reynolds number is held the same as that of the actual methane jet. The following word of caution is in order: The discussions on entrainment velocity fluctuations are qualitative since the temperature will be high in actual situation where the flame is established. Moreover, the transport properties of the product species will be different than that of the unburnt jet considered here. The data is acquired at the rate of 10 kHz, and the FFT analysis is done using MATLAB. Figure 3 shows the spectra of the entrainment velocity signals for jets evolving from burner vibrated with 1 mm amplitude and various frequencies. The static (non-vibrating) case is also shown in Fig. 3(a). Similar spectra are obtained for other amplitudes also, and it is observed in all the cases that the input vibration frequency dominates the velocity spectra. This confirms the fact that frequency of entrainment velocity oscillations closely follows that of the input vibration in the burner. However, in the cases of frequencies of 20 Hz and 30 Hz, smaller secondary peaks at frequencies higher than the input vibration frequency are also observed.

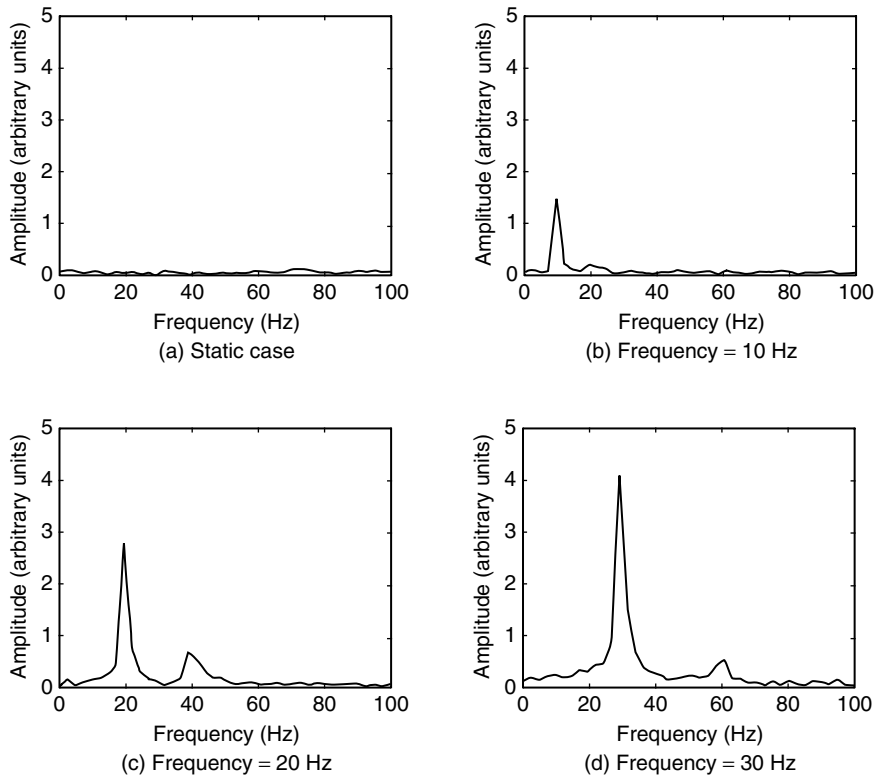

Figure 3: Spectra of velocity signals for (a) the static case and (b, c, d) for various frequencies of vibrations with 1 mm amplitude.

3.2. Flame oscillations

Methane is supplied to the burner with a constant mass flow rate of 1.39×10^{-6} kg/s. After a steady flame is established, the burner is excited with vibrations of various amplitudes and frequencies. For each case, including the non-vibrating case, high speed videos of direct flames and shadowgraph images are acquired at 300 fps using the high-speed camera, as mentioned before. Figure 4 show the instantaneous grayscale photographs extracted from the high speed video at regular time intervals of around 10 ms for burner vibration frequency of 10 Hz and amplitude 1 mm. These correspond to one cycle of burner vibration. An instantaneous photograph of flame from static burner is also shown in Fig. 4(a). Figure 7(a) shows the corresponding instantaneous shadowgraph images for the same case.

For this case, the characteristic fuel residence time given by the ratio of mean flame height (as observed in the static case) to the mean jet exit velocity is around 0.12 s. When the burner moves up, the entrainment velocity decreases (as the burner movement and the principal component of entrainment velocity are in same direction), and as a result,

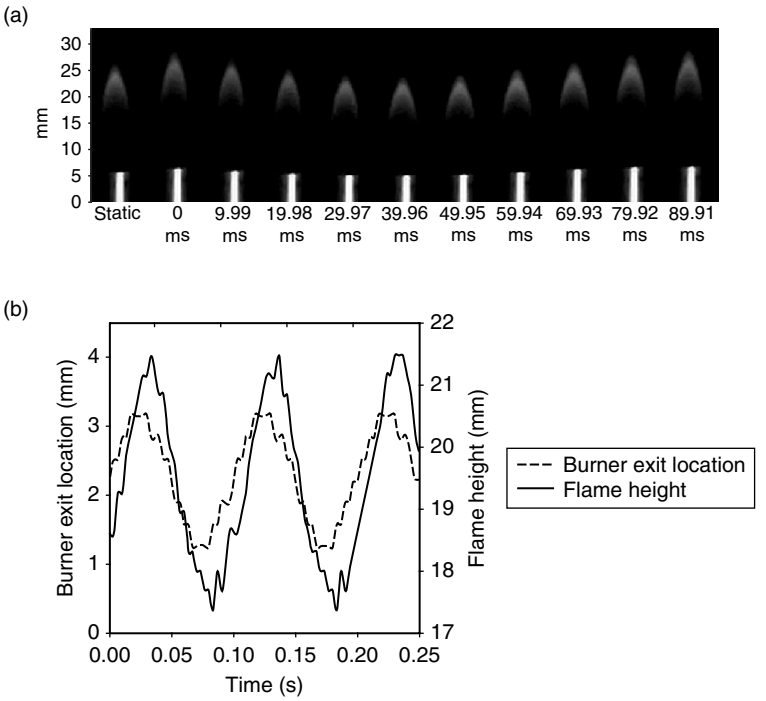

Figure 4: (a) Instantaneous photographs of flames and (b) time history of flame height and burner exit of the burner vibrated with frequency 10 Hz and amplitude 1 mm in comparison with static case.

the fuel jet travels longer to mix with stoichiometric amount of air. Therefore, as the burner moves upward, the entrainment rate decreases, and the flame height increases as shown in Fig. 4(a) (69.93–89.91 ms). Thus, when the burner reaches its uppermost point, the flame attains its maximum height. For a low frequency of 10 Hz burner vibration, the vibration time scale of 0.1 s closely matches that of the flow residence time scale (0.12 s) leading to oscillations of the flame envelope synchronous with the burner. Moreover, the diffusion time scales are negligible when compared to the flow time scales. In summary, if the vibration time scale matches the flow residence time scale, the flame oscillates almost in phase with the burner oscillations.

There is a time lag between the flame height oscillations and burner vibrations. Figure 4(b) shows the time history of flame height along with burner exit location for 10 Hz case. The flame height oscillations have a phase lag of 42 degrees with burner vibrations. This lag is due to inertia of the fluid.

As the burner continues to move downward, the flame becomes shorter due to further increase in the entrainment rate of the ambient air as shown in Fig. 4(a) (9.99– 49.95 ms).

The width of the flame slightly increases as more amount of fuel is burnt in a relatively shorter length due to increased entrainment. When the burner reaches the bottom most point, the corresponding flame becomes the shortest and the cycle continues.

However, when the frequency is increased to 20 Hz, a contrasting trend is observed. For the 20 Hz case, the characteristic fuel residence time remains the same, i.e., 0.12 s. However, the vibration time scale is now 0.05 s, which is much smaller than the fuel residence time. Therefore, for this case, there is a phase mismatch between the flame height response and the burner vibration. This is clearly shown in Fig. 5, where the instantaneous grayscale photographs at time intervals of 6.66 ms are shown for a vibration frequency of 20 Hz and amplitude of 1 mm. The flame height is the shortest when the burner location is at its maximum height from the mean position (Fig. 5, 26.64 ms) and is the longest when the burner is at its bottom-most point (Fig. 5, 0 ms).

The same trend is observed in the case of higher vibration frequency of 30 Hz due to further reduction in the vibration time scale to 0.0333 s, while the fuel residence time scale remaining constant at 0.12 s. Figure 6 shows the instantaneous grayscale photographs at time interval of 3.33 ms are shown for the case of vibration frequency of 30 Hz and amplitude of 1 mm. Figure 6 (0 ms) represents the minimum burner position having maximum flame height and Fig. 6(a) (13.32 ms) represents the maximum burner position and minimum flame height.

Figure 6(b) shows the time history of flame height along with burner exit location for 30 Hz case. The flame oscillations are almost out of phase with burner vibrations. The phase lag is found to be 216 degrees (180 + 36). This phase lag is found to increase with increase in frequency. Figure 9(b) shows the phase difference as a function of frequency. As the frequency is increased from 10 Hz to 15 Hz a sudden change in phase difference is observed (from 42 to 163 degress). Further increase in frequency also increases the phase difference significantly. The amplitude of vibration is found to have less effect on the phase difference.

When the burner starts moving upward from its lowest position, the burner rim velocity shifts its direction. As a result, the entrainment velocity relative to the burner exit increases as it is now almost out of phase with the burner vibrations (quite opposite to

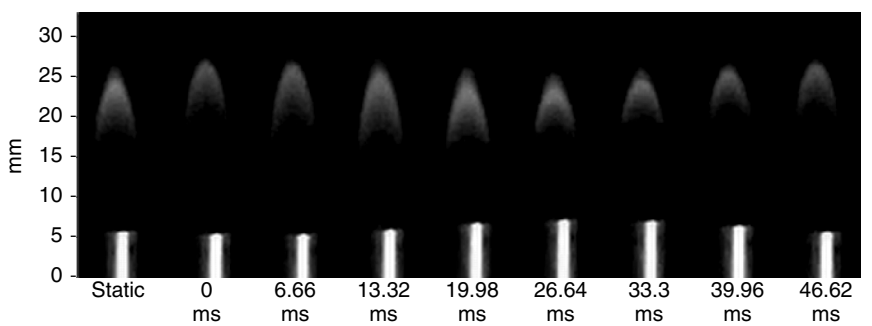

Figure 5: Instantaneous photographs of flame vibrated with frequency 20 Hz and amplitude 1 mm in comparison with static case.

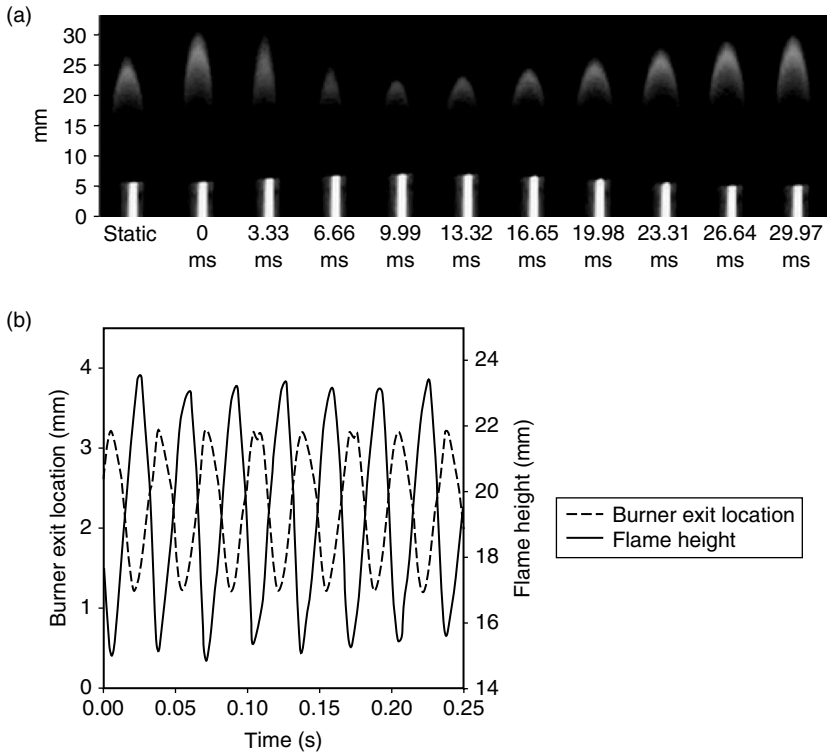

Figure 6: (a) Instantaneous photographs of flames and (b) time history of flame height and burner exit of the burner vibrated with frequency 30 Hz and amplitude 1 mm in comparison with static case.

the 10 Hz case). This increase in entrainment, however, does not immediately reduce the flame height, and there is a small time lag. This feature can be reasoned as follows. Even though the entrainment velocity is increased near the burner exit, still the fuel molecules in the fuel rich zones near the axis of the burner have to travel longer to reach the stoichiometric amount of air, as the change in entrainment has not been convected up to the flame height yet, when the burner has just started moving up. Therefore, the flame height does not decrease immediately. However, the flame radius is found to decrease when the burner just starts moving up. This phenomenon is explained as follows: There is a small partially premixed flame front formed in the periphery near to the burner exit, due to mixing of fuel with fresh air entraining at those locations. This portion of the flame is not visible in high-speed photographs due to its inadequate luminosity. This partially premixed zone is fuel-rich. Also, the inner core comprises mainly the fuel. When the burner starts moving upward, more air entrains in to the fuel jet base, and the fuel-rich partially premixed zone becomes leaner. Due to this the laminar burning velocity (S_L) increases, and more amount of fuel is consumed in this

small partially premixed zone. This results in reduced amount of fuel being transported to the non-premixed zone along the periphery of the jet flame. A similar trend is reported in Mohammad et al. [7].

3.3. Shadowgraph visualization

In order to visualize the dynamics of the diffusion flame structure, shadowgraph visualization of the flames is performed. In the shadowgraph images, the black region shows the burner shadow (Fig. 7). The maximum intensity (white) lines show the preheat regions in the air (outer white lines) and fuel sides (inner white cone). It is known that when the mixing is enhanced, the preheat line moves away from the flame surface because of the enhanced transport of heat towards the unburnt fuel and air side [19, 20]. Fig. 7(a) shows the shadowgraph images for frequency 10 Hz and amplitude 1 mm. The location of preheat line with respect to the burner exit is almost identical in all the frames.

The shadowgraph images for frequency 30 Hz and amplitude 1 mm is shown in Fig. 7(b). As the burner moves upward, the maximum intensity line moves downward relative to the edge of the burner exit, as shown in Fig. 7(b) (0–13.32 ms). This shows that the preheat zone moves downward and this is due to enhanced mixing [19, 20]. During this time period, reduction in flame height is observed in Fig. 6(a). As the burner moves downward, the maximum intensity line moves upward relative

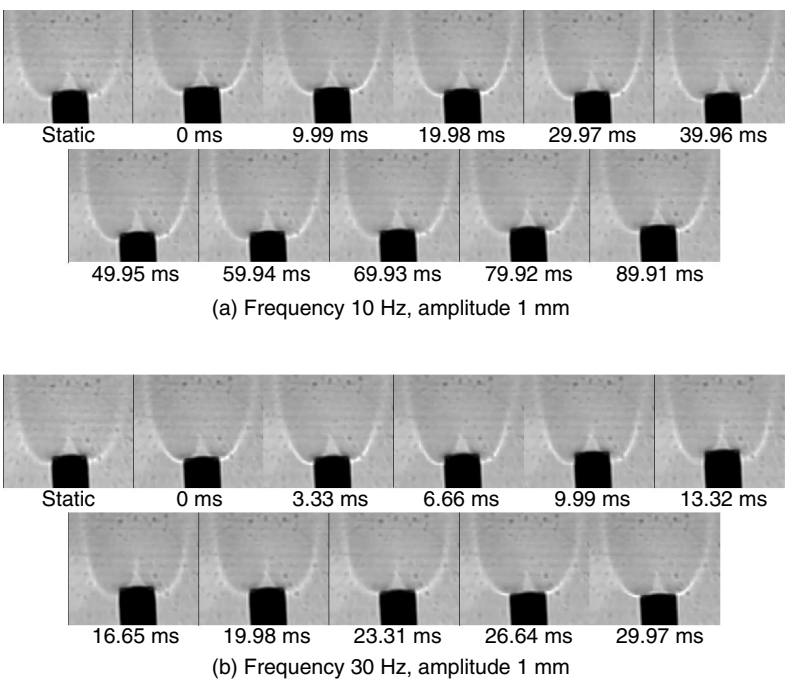

Figure 7: Instantaneous shadowgraphs of flames from static and vibrating burners.

to the edge of the burner exit, as shown in Fig. 7(b) (16.65–29.97 ms). During this time period, increasing trend in flame height is observed in Fig. 6(a). However, even though the movement of preheat line away from the burner exit is gradual as the burner moves upward [Fig. 7(b) (0–13.32 ms)], the movement towards the burner exit is an almost sudden when the burner just starts moving downward [Fig. 7(b) (16.65–19.98 ms)].

3.4. Flame height analysis

As mentioned in section 2, the flame heights are derived from the grayscale images. The flame heights represent the distance between the upper-most visible flame and the burner edge. Figure 8 shows the temporal variations of flame heights at different vibration amplitudes at the frequency of 30 Hz. It is clear from Fig. 8 that at a given frequency, as the amplitude of vibration is increased the amplitude of flame height oscillations increases.

For a better understanding of the flame response, a quantity termed as amplitude gain factor (G) is defined. 'G' is defined as the ratio of the amplitude of flame height (A_f) to the amplitude of input vibration (A_0). The flame response curve showing the variation of G with frequency of vibration is presented in Fig. 9 (a). It is clear that G monotonically increases with frequency, emphasizing the fact that frequency is a key parameter for flame height control.

Figure 10 shows the variation of the mean flame height (L_{mean}) as a function of A_0 for various frequencies of burner vibrations. The mean flame height is calculated by averaging the flame height over several oscillation cycles. It is clear that vibrations cause the mean flame heights to increase. However, the changes are minimal for smaller vibration amplitudes and frequencies. Larger flame oscillations occur at higher frequencies and higher amplitudes, within the range of values considered in this study.

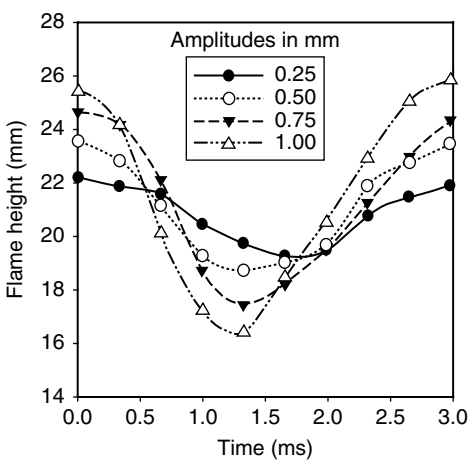

Figure 8: Variation of flame height in one cycle, vibrated with frequency 30 Hz and various amplitudes.

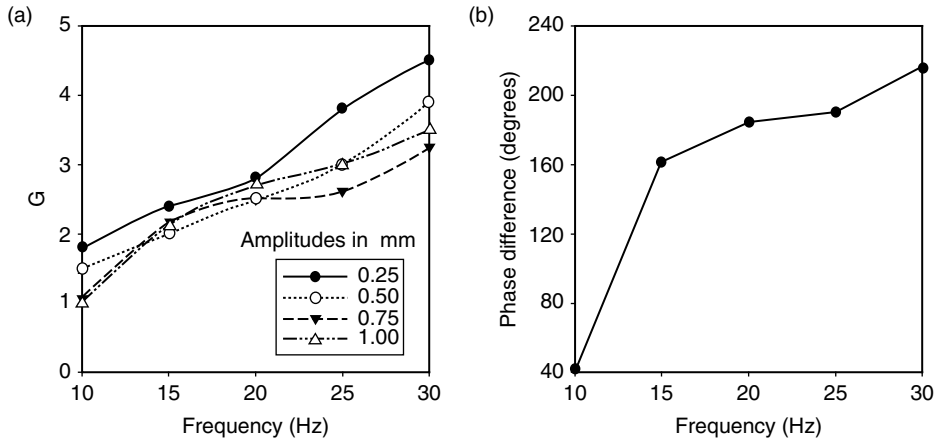

Figure 9: (a) Amplitude gain factor (G) for various frequencies and amplitudes (b) Phase difference between flame height oscillations and burner vibration for various frequencies for a constant amplitude of 1 mm.

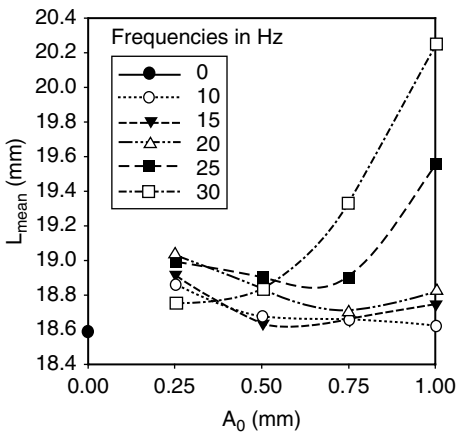

Figure 10: Mean flame height for various frequencies and amplitudes.

This trend is supported by the results reported in Albers et al. [3]. It should be noted that flame height analysis is only the first step towards understanding the flame dynamics. Advanced non-linear analysis, as in Ghosh et al. [27] could reveal other interesting facets of flame dynamics and their non-linear behaviour.

Albers et al. [3] reported the mean temperature profiles of modulated flames to be similar to that of the steady diffusion flame. However, the high frequency and high amplitude cases have higher mean flame heights when compared to static case and low frequency and low amplitude cases. This is due to fact that even though the flame

height does change continuously with respect to time in these cases, the increasing and decreasing trends are not similar. For instance, the flame height is almost constant in first three frames as shown in Fig. 6(a) (0–9.99 ms), it decreases as shown in Fig. 6(a) (9.99–16.65 ms), and gradually increases as shown in Fig. 6(a) (16.65–29.97). The flame has an above-average height for longer time when either the vibration frequency or its amplitude is higher. In Mohammad et al. [7], the reported CH radical concentration contours show a behavior similar to the above trend.

Figure 11 shows the spectra of flame height oscillations (measured with respect to instantaneous burner exit location) for two frequencies. At a lower frequency of 10 Hz, when the amplitude is less, the flame height oscillations take place predominantly with the input frequency. However as the amplitude is increased to 1 mm, very small peaks at harmonic frequencies are found. This is clearly shown in Fig. 11(a). Fig. 11(b) shows the frequency response of flame height oscillations for 30 Hz case. While the response shows predominantly the input frequency, the harmonics also found to exist significantly in high amplitude cases.

Figure 12 shows the spectra of intensity oscillations along axial (a, b) and radial (c, d) directions for two different frequencies and a constant amplitude of 1 mm. The axial spectra show that the oscillations in intensity are severe just above the flame height obtained in the static case (18.6 mm). But in 10 Hz case the oscillations are felt significantly in locations below this height. Harmonics are present in both the cases. Radial variation of intensity is also plotted at an axial location z = 23 mm, where maximum amplitude of intensity variation is reported along the axis. Fig 12(c) and Fig 12(d) show that the intensity oscillations are significant up to 1.5R from the axis of the burner, and the amplitude of oscillations are almost constant up to 1R.

3.5. Effect of flow rate

Diffusion flame height at steady conditions and in laminar regime depends only on the flow rate of the fuel. In order to examine the effect of variation in fuel flow rates for vibrating cases, two more fuel flow rates (1.95×10^{-6} kg/s and 2.50×10^{-6} kg/s) are considered in addition to 1.39×10^{-6} kg/s. Figure 13 shows the instantaneous

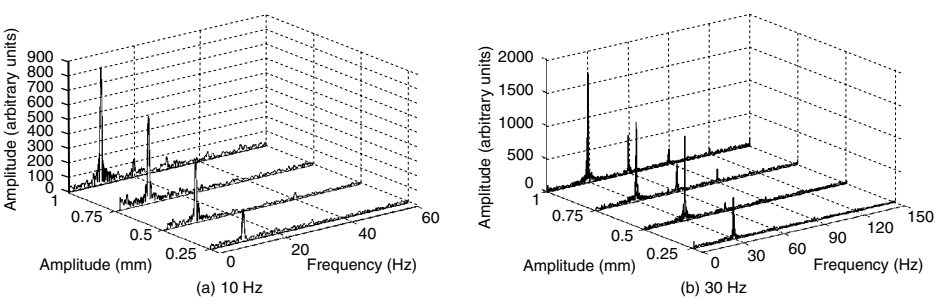

Figure 11: Frequency response of flame height oscillations for various input vibration amplitudes.

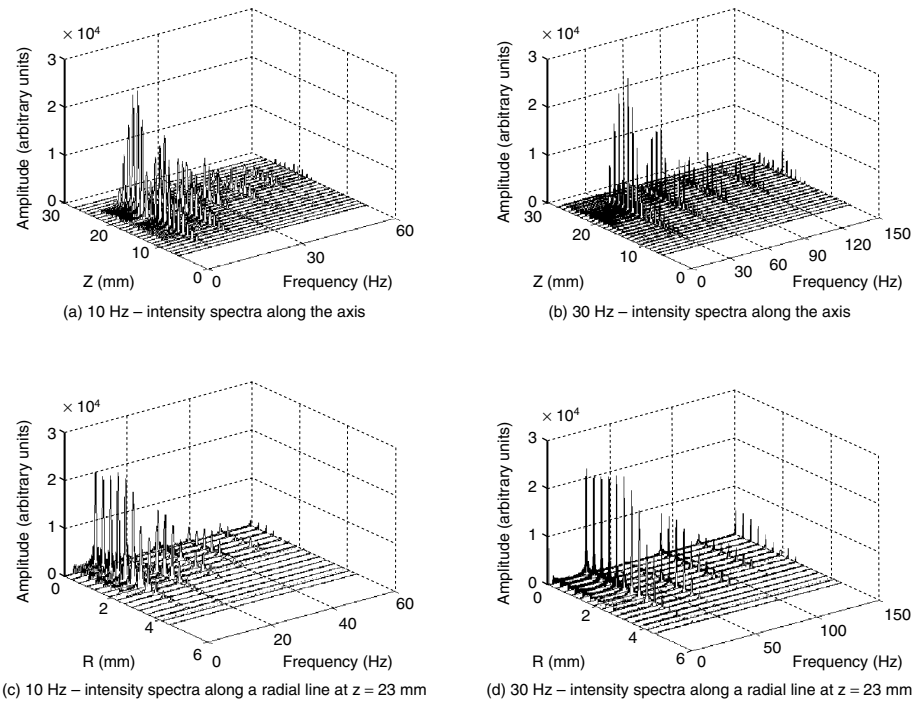

Figure 12: Spectra of flame intensity oscillations for 1 mm amplitude vibration.

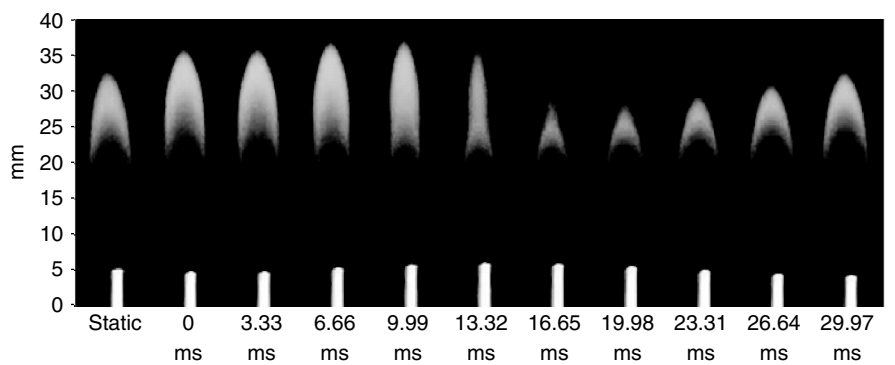

Figure 13: Instantaneous photographs of flame vibrated with frequency 30 Hz and amplitude 1 mm in comparison with static case, for fuel flow rate of 1.95×10^{-6} kg/s.

photographs of flames for a higher fuel flow rate of 1.95×10^{-6} kg/s. The trend is same as that in Fig. 6(a), however, with more clear view of instantaneous changes in both axial and radial extents.

In the flame height decreasing phase, upward movement of an entrainment vortex is shown by the response of flame shape. As the vortex moves upwards, the flame height suddenly reduces to its minimum and then gradually increases its mean height and towards the maximum value. These photographs are similar to the isotherms reported in Mohammad et al. [7].

The response of the taller flames to the burner vibration is more than that of the shorter flames. This is due to the decrease in the ratio of the length of local premixed region near the burner exit to the total length of the flame as the flames grow taller. A flame which is controlled predominantly by diffusion process is vulnerable to change in the entrainment.

3.6. Stability characteristics of turbulent diffusion flames

Several industrial burners operate in turbulent regimes. As the fuel flow rate is increased, the diffusion flame becomes turbulent and continued increase of fuel flow rate will result in the flame being lifted-off from the burner rim. According to Takahashi et al. [15, 16], the critical limits of stability are dependent predominantly on the geometry of the burner such as the burner rim thickness and flow configuration, although these limits are also affected by the type of fuel to some extent. In this section, flame lift-off characteristics in a vibrating burner are presented.

In the same experimental setup, methane is supplied at higher flow rates. After establishing a steady laminar diffusion flame, the flow rate of the fuel is increased gradually. At some fuel flow rate, the flame lifts-off from the burner rim. This flow rate corresponds to critical flow rate denoting initial flame lift-off; the corresponding velocity is termed as initial lift-off velocity (V_{LO}). As the process of lift-off is highly rapid, this experiment is repeated at least 5 to 6 times to ensure that the value of the initial lift-off velocity is consistent and repeatable. At this point, a high definition video is taken for a period of 4 s without changing the flow rate. This is to capture the initial lift-off height (h_{LO}).

Then the fuel flow rate is gradually reduced. As the flow rate reduces the lifted flame base slowly approaches the burner exit. At some flow rate, the flame attaches to the burner rim. This process also happens abruptly. The corresponding flow rate of methane in noted down as reattachment flow rate from which the reattachment velocity (V_{RA}) is calculated. These are repeated several times and the flow rate values are found to be within ±3%. The same procedure is repeated for various values of frequencies and amplitudes of burner vibrations.

Hotwire anemometry is performed near the burner exit at the burner exit plane (z = 0) at a radial location of r = 2.25D from the axis of the burner. The spectra are similar to those in Fig. 3, and hence not shown. However, for these higher flow rates, only one dominant peak is found (at the input vibration frequency), as opposed to a secondary peaks (at harmonic frequencies) observed for low flow rate cases shown in Fig. 3 (c & d).

Figure 14 shows the effect of burner vibration on the initial lift-off and reattachment velocities. For the static case, initial lift-off occurs around a fuel exit velocity of 17.3 m/s [Fig. 14(a)]. At low vibration amplitudes, as the frequency of burner vibration is

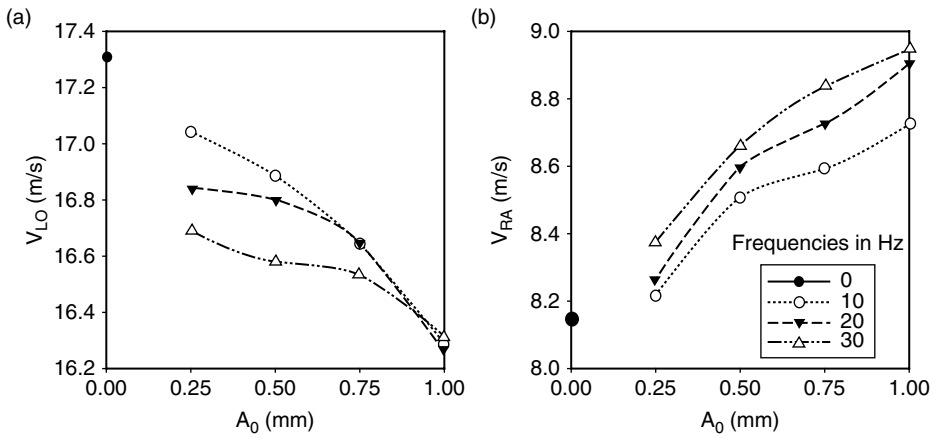

Figure 14: (a) Initial lift-off and (b) reattachment velocities for various frequencies and amplitudes.

increased, the initial lift-off occurs at lower fuel exit velocities. As the amplitude of vibration is increased, the difference between the initial lift-off velocities for various frequencies becomes lesser, finally converging to a value of 16.3 m/s at 1 mm amplitude. Takahashi et al. [16] reported that the lift-off velocity decreases when co-flow is introduced. This observation provides the rationale for the present observations. That is, under vibrating conditions, the entrainment is augmented during one half of the cycle. Since flame lift-off has a strong temporal dependence, the moment when entrainment is augmented, local quenching occurs, leading to instantaneous flame lift-off.

The effect of vibration on reattachment velocity is shown in Fig. 14(b). Reattachment velocity increases with increase in amplitude or frequency of burner vibration. This is due to the same reasons as discussed for lift-off velocity variations. While lift-off velocity reduction is due to the peak positive amplitude of entrainment velocity oscillations, the reattachment velocity increase is due to the peak negative side amplitude of entrainment velocity oscillations in any cycle of vibration. It is clear that the lift-off velocity decreases and reattachment velocity increases with increase in amplitude or frequency of burner vibration. This means that the hysteresis length reduces with increase in frequency or amplitude of burner vibrations.

As the flame lifts-off, it becomes unsteady and oscillates about a mean position above the burner rim. The mean lift-off height is calculated by averaging the instantaneous lift-off heights from the high speed video images. Figure 15 shows the variation of mean lift-off height for various amplitudes and frequencies of burner vibrations. The initial lift-off height for the static case is around 16.4 mm. For low vibration amplitudes, as the frequency is increased, the mean lift-off height significantly decreases. For a stable lifted flame, the lift-off height increases with increase in fuel jet exit velocity according to Pitts [18]. Thus, although the initial lift-off velocity is lower for vibrating cases, the

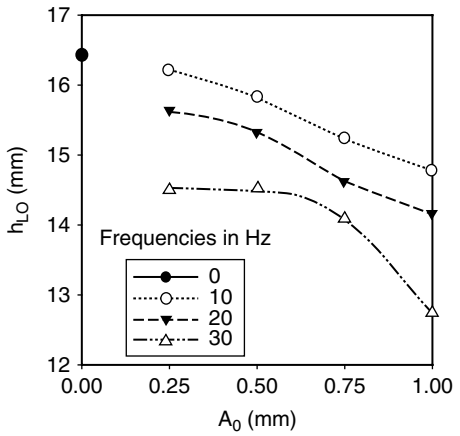

Figure 15: Lift off height for various frequencies and amplitudes.

lift-off heights are smaller than the static case. As a result, the burner operation range can be enhanced (postponing blow-off) using vibration as the active control tool. At the highest frequency considered, the lift-off height is seen to be the minimum at the highest amplitude of 1 mm. Further, when the fuel flow rate is increased so that the exit velocity is around 31.5 m/s, much higher than the initial lift-off velocity, the lift-off heights in mm for static and vibrating cases with an amplitude of 1 mm and frequencies 10 Hz, 20 Hz and 30 Hz, are found to be 135.6, 112.7, 112.6 and 108.1, respectively. This shows that the vibrations imparted to the burner increases its operating range. Therefore, it can be concluded that the primary effect of the burner vibrations is to increase the stability of a turbulent jet diffusion flame.

4. CONCLUSIONS

Mechanical vibrations introduced in diffusion flame burners significantly affect the combustion characteristics of the flames. Characteristics of laminar diffusion flames on an axially vibrating burner are studied for various frequencies and amplitudes of burner vibrations. Digital flame images from high-speed camera are presented along with shadowgraph images. It is observed that the oscillations in visible flame height due to harmonic vibration imparted to the burner are not sinusoidal. The amplitude of oscillation in flame height is found to increase with increase in both the frequency and the amplitude of burner vibration. The frequency of flame height oscillations is observed to be approximately the same as that of the burner. The flame height oscillations show a phase difference with the burner vibration for frequencies higher than approximately 10 Hz due to the reduction in the vibration time scale as compared to the fuel residence time scale. Effect of flow rate on the flame height oscillations is also presented; as flow rate increases the amplitude gain factor, which is the ratio of the amplitude of flame height oscillation to the amplitude of burner

vibration, also increases. As vibration is introduced in the burner, the velocity of the fuel jet at which the flame lifts-off, called the initial lift-off velocity, decreases. The lift-off velocity decreases with an increase in frequency or amplitude of the burner vibration, however, it is seen to be more influenced by the amplitude of vibration. At the highest amplitude of 1 mm considered in this study, the lift-off velocity reaches almost constant value irrespective of the frequencies. The initial flame lift-off height decreases with an increase in the frequency or amplitude of the burner vibration. The maximum percentage decrease in the lift-off height between the static and vibrating cases is much higher when compared to the maximum decrease in the lift-off velocity. Therefore, it is expected that the blow out may be postponed due to the vibrations introduced in the burner. Therefore, it can be concluded that the vibrations render a stabilizing effect on jet diffusion flames, and thus hold promise as an active control mechanism.

The relationship between entrainment in an actual flame and its dynamics, linear limits and non-linear flame dynamics offer scope for further work on this interesting and challenging topic of vibrated flames.

ACKNOWLEDGEMENTS

The authors sincerely acknowledge the funding from Aeronautics Research and Development Board, India for this work.

REFERENCES

[1] K. B. M. Q. Zaman and A. K. M. F. Hussain, Vortex pairing in a circular jet under controlled excitation. Part 1. General jet response, Journal of Fluid Mechanics, 1980, 101–3, 449–491.

[2] G. J. Nathan, J. Mi, Z. T. Alwahabi, G. J. R. Newbold and D. S. Nobes, Impacts of a jet's exit flow pattern on mixing and combustion performance, Progress in Energy and Combustion Science, 2006, 32, 496–538.

[3] B. W. Albers and A. K. Agrawal, Schlieren analysis of an oscillating gas-jet diffusion flame, Combustion and flame, 1999, 119, 84–94.

[4] A. Hamins, J. C. Yang and T. Kashiwagi, An experimental investigation of the pulsation frequency of flames, Twenty-fourth symposium (international) on combustion/the combustion institute, 1992, 1695–1702.

[5] A. J. Grant and J. M. Jones, Low-frequency diffusion flame oscillations, Combustion and flame, 1975, 25, 153–160.

[6] F. Aguerre, N. Darabiha, J. C. Rolon, and S. Candel, Fizika Goreniya i Vzryva, Experimental and numerical study of transient laminar counterflow diffusion flames, Fizika goreniya i vzryva, 1993, 29, No. 3, 61–66.

[7] R. K. Mohammed, M. A. Tanoff, M. D. Smooke, A. M. Schaffer And M. B. Long, Computational and experimental study of a forced, time-varying, Axisymmetric, laminar diffusion flame, Twenty-Seventh symposium (international) on combustion/the combustion institute, 1998, 693–702.

[8] S. B. Dworkin, B. C. Connelly, A. M. Schaffer, B. A. V. Bennett, M. B. Long, M. D. Smooke, M. P. Puccio, B. McAndrews, J. H. Miller, Computational and experimental study of a forced, time-dependent, methane–air coflow diffusion flame, Proceedings of the Combustion Institute, 2007, 31, 971–978.

[9] C. R. Shaddix, J. E. Harrington, and K. C. Smyth, Quantitative measurements of enhanced soot production in a flickering methane/air diffusion flame, Combustion and flame, 1994, 99, 723–732.

[10] C. R. Shaddix and K. C. Smyth, Laser-induced incandescence measurements of soot production in steady and flickering methane, propane, and ethylene diffusion flames, Combustion and flame, 1996, 107, 418–452.

[11] M. Saitoar, M. Sato and A. Nishimura, Soot suppression by acoustic oscillated combustion, Fuel, 1998, 77, No.9/10, 973–978.

[12] M. Charwath, J. Hentschel, H. Bockhorn and R. Suntz, Behavior of moderately oscillating sooting methane-air diffusion flames, Flow turbulence combust, 2009, 82, 553–569.

[13] K. C. Smyth, J. E. Harrington, E. L. Johnsson and W. M. Pitts, Greatly enhanced soot scattering in flickering CH_4 / Air diffusion flames, Combustion and flame, 1993, 95, 229–239.

[14] Y. Chao and M. Jeng, Behavior of the lifted jet flame under acoustic excitation, Twenty-fourth symposium (international) on combustion/the combustion institute, 333–340, 1992.

[15] F. Takahashi, M. Mizomoto, S. Ikai, and N. Futaki, Lifting mechanism of free jet diffusion flames, Twentieth symposium (international) on combustion/the combustion institute, 1984, 295–302.

[16] F. Takahashi and W. J. Schmoll, Lifting criteria of jet diffusion flames, Twenty-third symposium (international) on combustion/the combustion institute, 1990, 677–683.

[17] W. M. Pitts, Importance of isothermal mixing processes to the understanding of lift-off and blowout of turbulent jet diffusion flames, Combustion and flame, 1989, 76, 197–212.

[18] W. M. Pitts, Assessment of theories for the behavior and blowout of lifted turbulent jet diffusion flames, Twenty-Second symposium (international) on combustion/the combustion institute, 1988, 809–816.

[19] N. Peters, The turbulent burning velocity for large-scale and small-scale turbulence, Journal of fluid mechanics, 1999, 384, 107–132.

[20] W. A. Guttenfelder, G. B. King, J. P. Gore, N. M. Laurendeau and M. W. Renfro, Hydroxyl time-series measurements and simulations for turbulent premixed jet flames in the thickened preheat regime, Combustion and Flame, 2003, 135, 381–403.

[21] M. S. Mansour, N. Peters and Y. Chen, Investigation of scalar mixing in the thin reaction zones regime using a simultaneous CH-LIF/Rayleigh laser technique,

Twenty-seventh symposium (international) on combustion/the combustion institute, 1998, 767–773.

[22] F. J. Weinberg, The shadowgraph of a flat flame, Proceedings of royal society London, – A, 1956, 235, 510–517.

[23] G. H. Markstein, Interaction of flame propagation and flow disturbances, Third Symposium on Combustion, Flame and Explosion Phenomena, 1950, 162–167.

[24] R. E. Petersen, and H. W. Emmons, Stability of laminar flames, Physics of Fluids, 1961, 4, 456–464.

[25] T. A. Ferreira and W. Rasband, ImageJ user guide – version 1.43, Centre for Research in Neuroscience, McGill University, Montreal, QC, Canada, 2010.

[26] M. Valk, Acoustic Power Measurements of Oscillating Flames, Combustion and Flame, 1981, 41, 251–260.

[27] S. Ghosh, S. Mondal, T. Mondal, A. Mukhopadhyay and S. Sen, Dynamic characterization of candle flame, 2010, 2:3, 267–284.